THE COMPANY OF
Biologists

RESEARCH ARTICLE

Opsin expression, physiological characterization and identification of photoreceptor cells in the dorsal rim area and main retina of the desert locust, *Schistocerca gregaria*

Fabian Schmeling[1], Motohiro Wakakuwa[2], Jennifer Tegtmeier[1], Michiyo Kinoshita[2], Tobias Bockhorst[1], Kentaro Arikawa[2] and Uwe Homberg[1,*]

ABSTRACT

For compass orientation many insects rely on the pattern of sky polarization, but some species also exploit the sky chromatic contrast. Desert locusts, *Schistocerca gregaria*, detect polarized light through a specialized dorsal rim area (DRA) in their compound eye. To better understand retinal mechanisms underlying visual navigation, we compared opsin expression, spectral and polarization sensitivities and response–stimulus intensity functions in the DRA and main retina of the locust. In addition to previously characterized opsins of long-wavelength-absorbing (Lo1) and blue-absorbing visual pigments (Lo2), we identified an opsin of an ultraviolet-absorbing visual pigment (LoUV). DRA photoreceptors exclusively expressed Lo2, had peak spectral sensitivities at 441 nm and showed high polarization sensitivity (PS 1.3–31.7). In contrast, ommatidia in the main eye co-expressed Lo1 and Lo2 in five photoreceptors, expressed Lo1 in two proximal photoreceptors, and Lo2 or LoUV in one distal photoreceptor. Correspondingly, we found broadband blue- and green-peaking spectral sensitivities in the main eye and one narrowly tuned UV peaking receptor. Polarization sensitivity in the main retina was low (PS 1.3–3.8). *V*–log *I* functions in the DRA were steeper than in the main retina, supporting a role in polarization vision. Desert locusts occur as two morphs, a day-active gregarious and a night-active solitarious form. In solitarious locusts, sensitivities in the main retina were generally shifted to longer wavelengths, particularly in ventral eye regions, supporting a nocturnal lifestyle at low light levels. The data support the role of the DRA in polarization vision and suggest trichromatic colour vision in the desert locust.

KEY WORDS: Compound eye, Dorsal rim area, Opsin expression, Spectral sensitivity, Polarization sensitivity, Phase change

INTRODUCTION

In addition to the position of the sun, many insects rely on the pattern of polarized light (POL) in the blue sky for spatial orientation (Horváth and Varjú, 2004; Wehner and Labhart, 2006; Homberg and el Jundi, 2014). Polarotactic orientation has been demonstrated in field experiments in the desert ant (Wehner and Müller, 2006), the honeybee (von Frisch, 1949), several species of dung beetles (Dacke et al., 2003; Dacke et al., 2011), the monarch butterfly (Reppert et al., 2004) and the fruitfly (Weir and Dickinson,

2012) and, in laboratory experiments, in the house fly (von Philipsborn and Labhart, 1990), the field cricket (Brunner and Labhart, 1987), and the desert locust (Mappes and Homberg, 2004). In all of these insects, POL detection is mediated by a small dorsal rim area (DRA) in the compound eye (Labhart and Meyer, 1999).

Ommatidia and photoreceptor cells in the DRA are highly specialized. DRA ommatidia contain homochromatic photoreceptors with high polarization sensitivity (PS) based on precisely aligned microvilli. In each ommatidium microvilli are oriented in two blocks orthogonal to each other (Labhart and Meyer, 1999). The DRA of the desert locust, *Schistocerca gregaria* (Forskål 1775), has about 400 ommatidia (Homberg and Paech, 2002). Each DRA ommatidium contains eight photoreceptor cells (R1–R8). The microvilli of R7 are oriented orthogonally to those of R1, R2, R5, R6 and R8, whereas the microvilli of R3 and R4 are small and less well oriented (Homberg and Paech, 2002).

Polarization vision pathways in the brain of *S. gregaria* have been studied particularly well (Homberg et al., 2011). Polarized light signals from the DRA are combined with chromatic contrast information from the sky in the anterior optic tubercle of the brain (Pfeiffer and Homberg, 2007), and signals from both eyes are integrated in the central complex, serving a probable role as an internal sky compass in the brain (Heinze and Homberg, 2007; Heinze et al., 2009).

Schistocerca gregaria occurs widely in North Africa and the Middle East, and exhibits two different morphological phases with strongly differing appearance and behaviour (Uvarov, 1966; Simpson et al., 1999). Swarm-building locusts of the gregarious phase perform long-distance migrations during the day, whereas the solitarious phase also migrates but is largely nocturnal (Roffey, 1963; Waloff, 1963; Roffey and Magor, 2003). While there is evidence for sky compass orientation in gregarious animals (Kennedy, 1951), the control of navigation in solitarious locusts is unknown.

In contrast to central processing of polarized light, the physiology of DRA photoreceptors in *S. gregaria* is poorly understood. Eggers and Gewecke (Eggers and Gewecke, 1993) reported blue-sensitive receptors with high PS values and UV receptors with low PS values in the DRA, but did not identify the photoreceptor cell types morphologically. Although two opsins, a long-wavelength opsin and a middle-wavelength opsin, have been identified in *S. gregaria* (Towner et al., 1997), no data exist on their distribution in the eye. We therefore reinvestigated the number and sequences of mRNAs encoding visual pigment opsins and their presence in the DRA of the locust. In addition, we studied spectral sensitivities, response–stimulus intensity (*V*–log *I*) functions and polarization sensitivity of DRA photoreceptors and identified the recorded cell type through dye injections. All data were compared with those from

[1]Fachbereich Biologie, Tierphysiologie, Philipps-Universität Marburg, 35032 Marburg, Germany. [2]Laboratory of Neuroethology, Sokendai (The Graduate University for Advanced Studies), Shonan Village, Hayama, Kanagawa 240-0193, Japan.

*Author for correspondence (homberg@biologie.uni-marburg.de)

The Journal of Experimental Biology
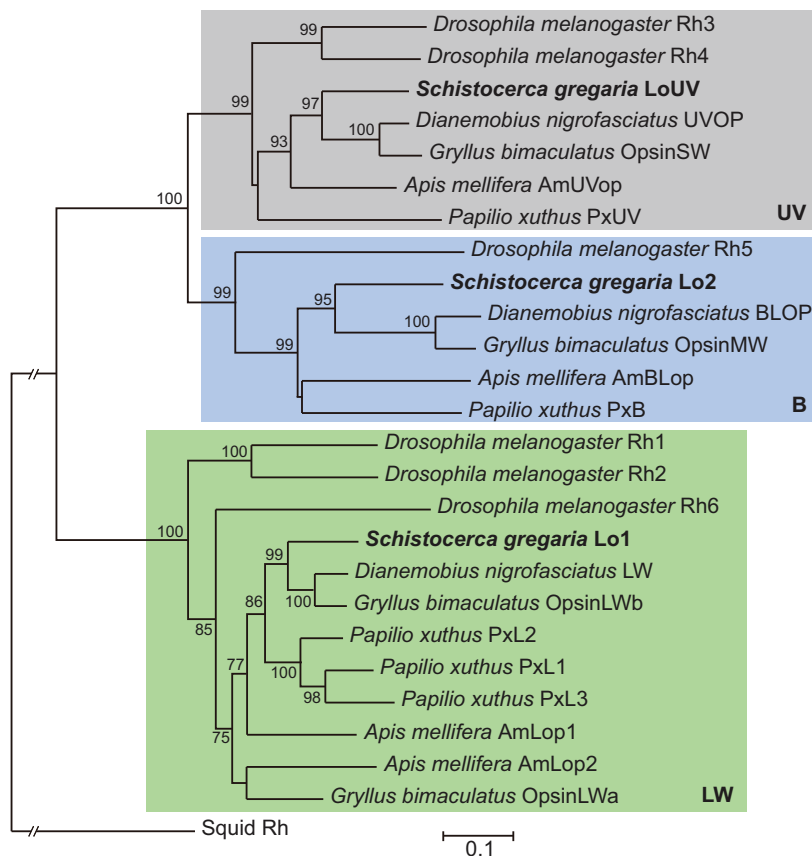
Fig. 1. Phylogenetic relationship of insect opsins of the UV, blue (B) and long wavelength (LW) type inferred by the neighbour joining method. Squid rhodopsin (Rh) was used as the outgroup. Numbers at the branches indicate bootstrap values based on 1000 replicate analyses. Values larger than 70% are shown. Accession numbers are as follows: *Drosophila melanogaster* Rh1, K02315; *D. melanogaster* Rh2, M12896; *D. melanogaster* Rh3, M17718; *D. melanogaster* Rh4, P08255; *D. melanogaster* Rh5, U67905; *D. melanogaster* Rh6, Z86118; *Schistocerca gregaria* LoUV, AB902953; *S. gregaria* Lo1, X80071; *S. gregaria* Lo2, X80072; *Dianemobius nigrofasciatus* UVOP, AB458852; *D. nigrofasciatus* BLOP, AB291232; *D. nigrofasciatus* LW, FJ232921; *Gryllus bimaculatus* OpsinSW, HM363623; *G. bimaculatus* OpsinMW, HM363622; *G. bimaculatus* OpsinLWa, HM363620; *G. bimaculatus* OpsinLWb, HM363621; *Apis mellifera* AmUVop, AF004169; *A. mellifera* AmBLop, AF004168; *A. mellifera* AmLop1, BK005514; *A. mellifera* AmLop2, BK005515; *Papilio xuthus* PxUV, AB028218; *P. xuthus* PxB, AB028217; *P. xuthus* PxL1, AB007423; *P. xuthus* PxL2, AB007424; *P. xuthus* PxL3, AB007425.

non-DRA regions, i.e. the main region of the eye. To uncover possible differences related to lifestyle, we compared data from gregarious and solitarious locusts.

RESULTS

Cloning of UV opsin cDNA

We cloned a cDNA encoding an opsin of an ultraviolet (UV)-absorbing visual pigment from poly-A RNA extracted from the compound eye. Phylogenetic analysis of the sequence we identified using the neighbour-joining method revealed that the cDNA sequence clusters in the UV wavelength-absorbing clade of insect opsins (Fig. 1). The desert locust, therefore, has at least three opsin genes, encoding a long wavelength (Lo1) and a blue-absorbing type (Lo2), which were identified previously (Towner et al., 1997), and a UV-absorbing type (LoUV).

Distribution of opsin mRNAs in the retina

We localized the LoUV, Lo1 and Lo2 mRNA in the retina by double-targeted *in situ* hybridization. We labelled transverse sections of distal and proximal tiers of the retina with probes specific to mRNAs encoding for the three opsins in all combinations (Fig. 2A–E). At the distal tier of the retina (Fig. 2A–C), R7 photoreceptors were labelled by either the LoUV (black arrowheads in Fig. 2A–C) or the Lo2 probe (white arrowheads). Labelling by the Lo2 probe in R7, which expressed solely Lo2, was stronger than that of the larger R2, R3, R5, R6 and R8 photoreceptors (white arrowheads in Fig. 2A). Interestingly, all other photoreceptor cells (R2, R3, R5, R6 and R8) in the distal tier were labelled by both the Lo1 and Lo2 probes in an overlapping manner (Fig. 2A,B). As a result, the appearance of double-labelled photoreceptors was dark red (Fig. 2C). R7 occurred at two different positions within the

ommatidia (Fig. 2A–C) but its position was not related to mRNA expression in R7. In the proximal tier (Fig. 2D,E), two additional photoreceptors, R1 and R4 (proximal photoreceptor cells) appeared, whereas R7 disappeared. R1 and R4 were labelled by the Lo1 probe exclusively (Fig. 1D,E, arrowheads). As well as in the distal tier, R2, R3, R5, R6 and R8 were labelled by both the Lo1 and Lo2 probe.

Longitudinal sections showed that the DRA (Fig. 2F–I, surrounded by the interrupted line) was only labelled by the Lo2 probe throughout the entire length of ommatidia. We did not find any labelled cells in the DRA with the LoUV and the Lo1 probes. The labelling pattern in the rest of the eye was rather constant, suggesting that there is no clear regionalization. R7 photoreceptors labelled by the LoUV probe were identified only in the distal retina (Fig. 2F, inset arrows), whereas Lo1 and Lo2 probe labelled throughout the entire length of the ommatidia. The fluorescence image of double labelling with Lo1 and Lo2 probes showed that green opsin (Lo2) was expressed throughout the main retina: the green-induced red fluorescence is due to the dye FastRed (see Materials and methods) (Fig. 2I).

Fig. 2J summarizes the expression of opsin mRNAs on transverse sections. The DRA consisted of only one type of ommatidium expressing the blue opsin mRNA in all photoreceptors. In the main eye, two types of ommatidia were distinguished in accordance with R7 either expressing the UV (type I: solid circle) or blue opsin mRNA (type II: broken circle), respectively (Fig. 2A–C). In both types of ommatidia, receptors R2, R3 and R5–R8 co-expressed blue (Lo1) and green (Lo2) opsin mRNAs, whereas the proximal receptors (R1, R4) contained only green (Lo2) opsin mRNA. The appearance of labelled photoreceptors at different depths of the ommatidia indicates that R7 is a distal photoreceptor, and R1 and R4 are proximal
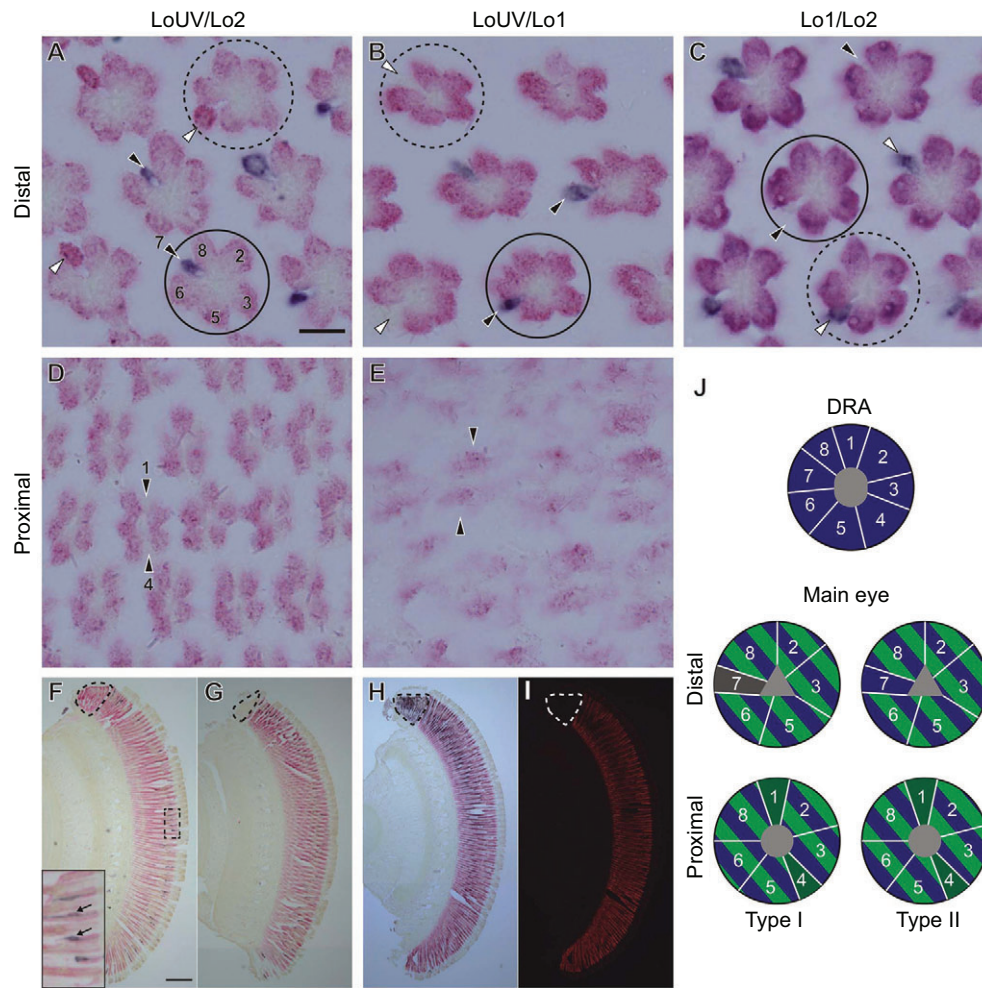
Fig. 2. Localization of opsin mRNAs by double label *in situ* hybridization. Transverse sections (A–E) and longitudinal sections (F–I) were labelled by probes specific to the LoUV (black) and the Lo2 (red) in A, D and F, the LoUV (black) and the Lo1 (red) in B, E and G, and Lo2 (black) and Lo1 (red) in C, H and I. H and I show the same section photographed under regular transmission light (H) and green epi-illumination (I). The distal transverse sections reveal two types of ommatidia indicated by solid circles (type I) and broken circles (type II) in A–C. Numbers in A and D indicate position of each photoreceptor. The distal photoreceptor R7 expresses either LoUV (black arrowheads in A–C) or Lo2 (white arrowheads in A–C). The proximal photoreceptors R1 and R4 (arrowheads in D,E) express only Lo1. The region surrounded by the broken line in transverse sections (F–I) is the DRA. Inset in F is the enlarged image of the distal tier (broken rectangle in F). The top and bottom of images in F–I are dorsal and ventral, respectively. (J) Diagram of *in situ* hybridization labelling patterns of ommatidia in the DRA and distal and proximal tiers of ommatidia in the main retina. In the DRA all photoreceptors express Lo2. In the main retina, the proximal photoreceptors R1 and R4 express Lo1, the distal photoreceptors R2, R3, R5, R6 and R8 co-express Lo1 and Lo2, whereas R7 expresses either LoUV (type I ommatidia) or Lo2 (type II ommatidia). Scale bars, 10 µm (A–E, shown in A) and 200 µm (F–I, shown in F).

photoreceptors. Type I and type II ommatidia were distributed randomly over the main retina in a ratio of 1.8:1.

Electroretinographic recordings

In electroretinographic (ERG) recordings from 28 locusts (13 gregarious and 15 solitarious animals) we investigated the spectral sensitivity of distinct eye regions (Fig. 3). Recordings from the DRA and the dorsal (DA) and ventral (VA) halves of the main retina in gregarious locusts supported the *in situ* hybridization results. The spectral sensitivity of the DRA showed a peak at 430 nm with a shoulder in the UV range at about 350 nm. At longer wavelengths beyond 430 nm, sensitivity decreased strongly, indicating the absence of long wavelength receptors. In the DA, the blue sensitivity peak remained the same, but the sensitivity bandwidth extended into longer wavelengths, indicating the presence of long wavelength-absorbing visual photopigments in the dorsal half of the main retina. Finally, in the VA peak sensitivities occurred broadly at around 350, 450 and 510 nm, indicating the presence of UV, blue and long wavelength-absorbing visual pigments.

The spectral sensitivity of the DRA did not differ between the two locust phases, but phase-dependent differences occurred in the DA and VA. In the DA of solitarious animals the peak sensitivity was slightly shifted to longer wavelengths (470 nm), suggesting a higher contribution of long wavelength receptors. In the VA of solitarious locusts the peak sensitivity was even further shifted into the green range (510–530 nm) and decreased strongly in the UV, suggesting low contribution of UV receptors.

Single-cell recordings

In intracellular recordings we investigated the spectral sensitivity, response–stimulus intensity functions, and polarization sensitivity of photoreceptors in the DRA (Fig. 4) and compared these data with recordings from the main eye (non-DRA receptors). Dye injection into the recorded cell allowed us to identify the photoreceptor within the DRA ommatidium (Fig. 4G).

Spectral sensitivity of single photoreceptors

Spectral sensitivity tested in recordings from over 100 gregarious and 24 solitarious locusts revealed three types of spectral receptors, peaking in the UV, blue or green region of the spectrum. Whereas only blue peaking cells were found in the DRAs of both phases, all three spectral types occurred in the main eye. In the main eye of gregarious locusts, peak sensitivities were found most frequently in the blue wavelength range around 410–450 nm and in the green spectrum at 530 nm. In solitarious locusts, likewise, peaks occurred in the long wavelength range around 530 nm but peaks in the blue spectrum were often shifted to longer wavelengths around 470 nm (Fig. 5).

Spectral recordings from the main retina were sorted into groups of 310–390 nm, 410–490 nm and 510–630 nm peak sensitivity. Averaged relative spectral sensitivities were calculated for those groups (Fig. 6). To estimate λ_{max} values and relative contributions of green and blue opsins in non-DRA photoreceptors, we fitted visual pigment absorption spectra to the absorbance spectra using the Govardovskii et al. (Govardovskii et al., 2000) template (Fig. 6).
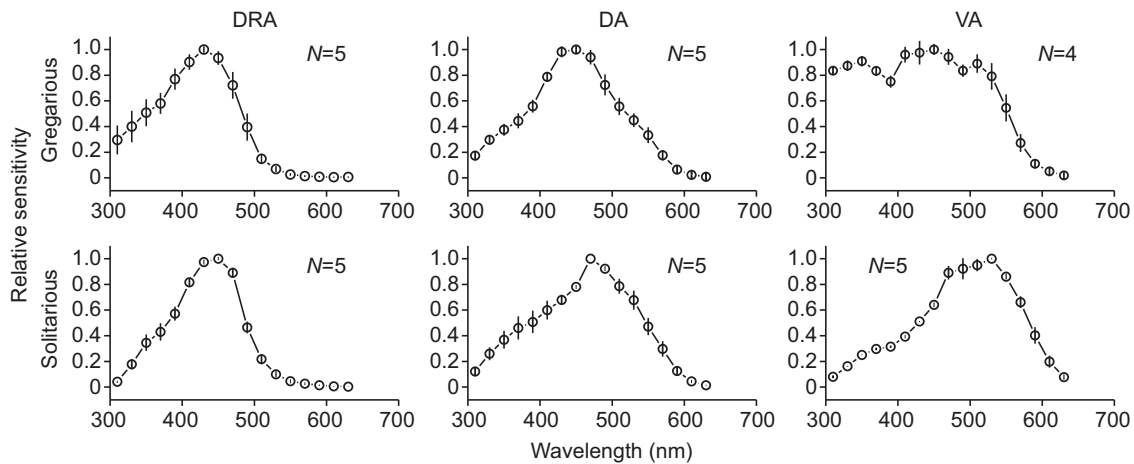
Fig. 3. ERG-determined spectral sensitivity curves from distinct eye regions in gregarious and solitarious locusts. Averaged data ± s.e.m. from ERG recordings in the DRA (N=5 animals, 23 and 21 recordings), and dorsal (DA; N=5 animals, 20 and 13 recordings) and ventral (VA; N=4 resp. 5 animals, 12 and 20 recordings) halves of the main eye. In both phases the DRA is mainly sensitive in the blue spectrum, whereas green sensitivity increases towards ventral eye regions. In the solitarious phase this green shift is more dominant than in the gregarious phase. In addition, the VA of gregarious animals shows high sensitivity in the UV.

The spectral sensitivities of the DRA blue receptors were best fitted by absorption spectra of a visual pigment with λ_{max} of 442 nm (Fig. 6A, gregarious locusts), resp. 437 nm (Fig. 6A′, solitarious locusts). Template fitting of the green peaking receptors yielded a λ_{max} of 516 nm (Fig. 6B, gregarious locusts), resp. 511 nm (Fig. 6B′, solitarious locusts), although with relatively low R^2 values. Poor matching with the template was especially obvious in the short wavelength range. Based on the *in situ* hybridization data suggesting co-expression of blue and green opsins in the main eye, we therefore fitted a mixture of blue and green templates based on the fitting results in Fig. 6A,B and 6A′,B′, respectively, to the green peaking spectra (Fig. 6C,C′). Best fits with improved R^2 values were obtained by a relative contribution of 16:84 (relative amplitude λ_{max} blue: λ_{max} green) for gregarious and 23:77 (blue:green) for solitarious locusts. Blue peaking receptors in the main eye region

(Fig. 6D,D′) were best fitted by a ratio of 90:10 (blue:green) for gregarious, and 46:54 (blue:green) for solitarious locusts. The UV receptor was best fitted by an absorption spectrum with λ_{max} of 339 nm (Fig. 6F). Because the confidence intervals of λ_{max} values for green and blue visual pigments showed considerable overlap between gregarious and solitarious locusts, suggesting that their opsins are identical, we pooled the data of DRA blue and non-DRA green-peaking receptors from both phases and obtained best fits with peak absorbances at 441 nm (R^2=0.96) for the blue and 514 nm (R^2=0.83) for the green opsin (Fig. 6F).

V–log I functions

Mean V–log I curves were determined for DRA receptors and green and blue peaking receptors of the main eye of both locust phases. In both phases, the V–log I curves of DRA receptors were shifted to
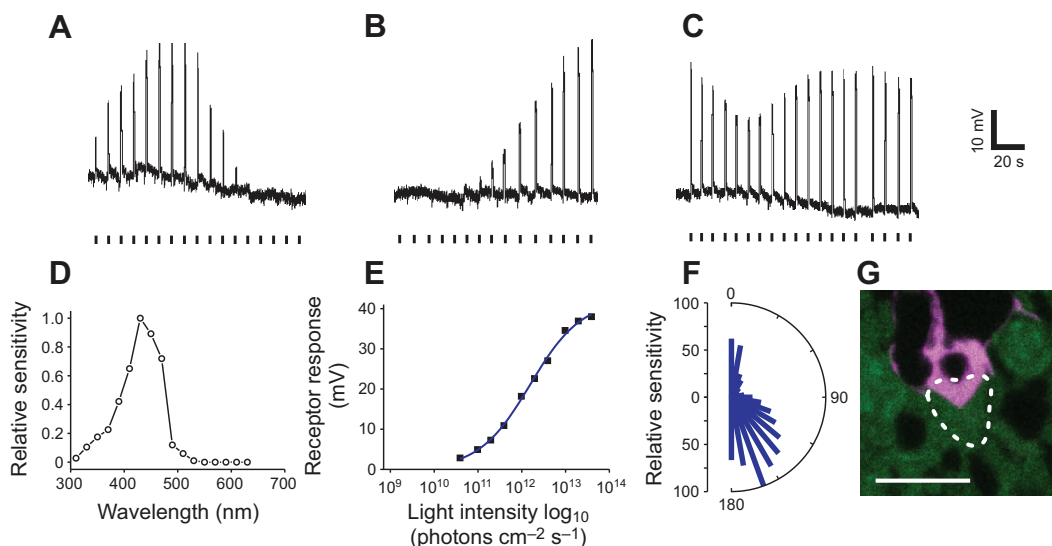
Fig. 4. Complete set of electrophysiological data from an R7 photoreceptor in the DRA. (A,D) Spectral sensitivity; (B,E) intensity response relationship; (C,F) polarization sensitivity. A–C show original recording traces and D–F the corresponding graphs. (A) Spectral testing was always the first step to determine receptor spectral type. (B) To calculate relative sensitivities the receptor response curve was measured with the wavelength causing the strongest receptor response (here 430 nm). (C) The same wavelength was used for POL testing. (G) Following tracer injection, the recorded photoreceptor was identified by fluorescence microscopy of ommatidial cross-sections. The white dotted line indicates the perimeter of the rhabdom (R). Scale bar, 5 μm.
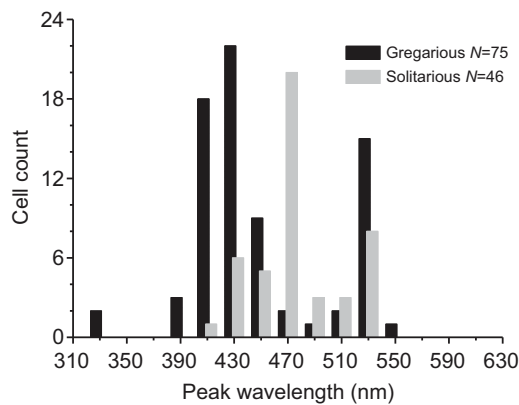
Fig. 5. Spectral sensitivity peaks in the main retina of gregarious and solitarious locusts. Data originate from single-cell recordings. Peak sensitivities occur around 430 and 530 nm in gregarious locusts. In solitarious animals peaks in the green are likewise around 530 nm, but in the blue are shifted towards longer wavelengths around 470 nm, indicating a difference in spectral sensitivity between the gregarious and solitarious phases.

higher light intensities (high K) and were steeper than the non-DRA curves (Fig. 7). To analyse possible differences in the relative sensitivities of DRA and non-DRA receptors, we compared two parameters of the V–log I functions: light intensity at half-maximal receptor excitation and the exponential slope (K and n in the Naka–Rushton equation). Blue peaking recordings from the DRA and blue- and green peaking recordings from the main retina (non-DRA) were grouped and compared with each other. Significant differences were found for K and n between the DRAs and main retinae, whereas the two locust phases did not differ from each other (Fig. 8).

K values did not differ statistically between DRA and non-DRA blue peaking receptors in gregarious and solitarious locusts, but in both phases they were significantly lower in non-DRA green peaking receptors than in DRA blue receptors. Values of n were significantly higher in both locust phases in DRA receptors compared with non-DRA receptors. No differences were found between blue peaking and green peaking cells in the main retina.

Polarization sensitivity

Polarization sensitivity was tested in 26 recordings from gregarious locusts and 43 recordings from solitarious locusts. During stepwise rotation of the polarizer, the amplitude of receptor responses was modulated sinusoidally as illustrated in the circular graphs in Fig. 9B,C,E. The strength of this modulation was calculated as the PS value. In gregarious locusts, PS values in the DRA ranged from 2.4 to 22.4 (N=16), confirming the role of DRA photoreceptors as detectors of polarized light (Fig. 9D). Dye injection showed that all eight receptors in DRA ommatidia had high PS values, despite differences in size and orientation of their rhabdomeres (Fig. 10). In contrast, PS values of non-DRA blue and green peaking receptors were well below 3 (non-DRA blue peaking receptors: PS=1.9–2.3, N=10; non-DRA green peaking receptors: PS=2–2.2, N=2; Fig. 9A).

In DRA photoreceptors of solitarious locusts, a higher number of PS values below 3 was found in addition to high values above 20 (DRA: range 1.3–31.7, N=9; Fig. 9D). The distribution of PS values in non-DRA photoreceptors was similar to that in gregarious locusts (non-DRA blue peaking receptors: PS=1.3–3.8, N=35; non-DRA green peaking receptors: PS=1.4–2.3, N=6; Fig. 9A). No test for polarization sensitivity was achieved for UV cells.

Cell identity

DRA photoreceptors of gregarious locusts were identified through neurobiotin injection. Cell numbering in DRA ommatidia of locusts is based on the position of crystalline cone threads (Homberg and Paech, 2002). Although these structures cannot be observed under confocal laser microscopy, another important landmark, photoreceptor R7, could be identified based on its position opposing the other photoreceptors in DRA ommatidia (Homberg and Paech, 2002). Data from right eyes were mirrored to fit to left eye conditions before cell numbering.

For further assurance that physiological responses originated from the actually stained cell, POL responses were compared with microvilli orientation, taking into account the position of the locust in the experimental setup. If E-vector orientation at maximum receptor response was identical with microvilli orientation of the labelled receptor cell, correct assignment of physiological and anatomical data was assumed. Further indicators for distinguishing receptors were position of the ommatidium in the DRA, size and orientation of cell body and rhabdomere and position of the stained cell within the ommatidium.

In the DRA of gregarious locusts, six of the eight photoreceptor cells could be identified by single-cell staining (R1=1, R2=6, R3=4, R6=2, R7=14, R8=2; Fig. 10). Staining of R4 (N=1) and R5 (N=1) included secondary fainter staining from other photoreceptor cells (for explanation, see Fig. 10).

DISCUSSION

We have characterized the functional organization of the DRA and the main retina in the desert locust through opsin gene expression, ERG and intracellular recordings. The data show that the DRA of the eye exclusively contains blue receptors with high polarization sensitivity. In the main retina of gregarious animals two types of ommatidia exist. Both types contain two proximal green receptors and five receptors that co-express blue and green opsins. The eighth receptor is a distal photoreceptor and expresses either blue or UV opsin. The two types of ommatidia are randomly distributed throughout the main retina. ERG and intracellular recordings revealed spectral sensitivities supporting the opsin gene expression data. Solitarious locusts differed from gregarious animals by a lower contribution of UV sensitivity in the ventral eye and an increase in green sensitivity throughout the eye.

Opsin expression and ommatidial organization

We identified a novel opsin of a UV-absorbing visual pigment (LoUV) in the retina of the desert locust, in addition to previously characterized (Towner et al., 1997) long wavelength (Lo1) and blue-absorbing types (Lo2). Desert locusts, therefore, have three distinct visual pigments like many other insect species (Briscoe and Chittka, 2001). We have predicted the possible absorbance spectra of these visual pigments based on the physiologically determined spectral sensitivities of photoreceptors. It thus appears that LoUV is a visual pigment (P) with an absorption peak at 339 nm (P339), Lo1 is a P514 and Lo2 is a P441. The distribution of opsin gene expression is strikingly different in the DRA and main retina. All photoreceptors of DRA ommatidia exclusively express the blue-sensitive Lo2, underscoring homochromacy throughout this polarization-sensitive eye region.

In contrast to the DRA, opsin gene expression in the main eye is not identical in all ommatidia. Ommatidial structure in the main eye is similar to that of the migratory locust *Locusta migratoria* (Wilson et al., 1978) with five photoreceptors (R2, R3, R5, R6, R8) contributing microvilli throughout the length of the rhabdom, a
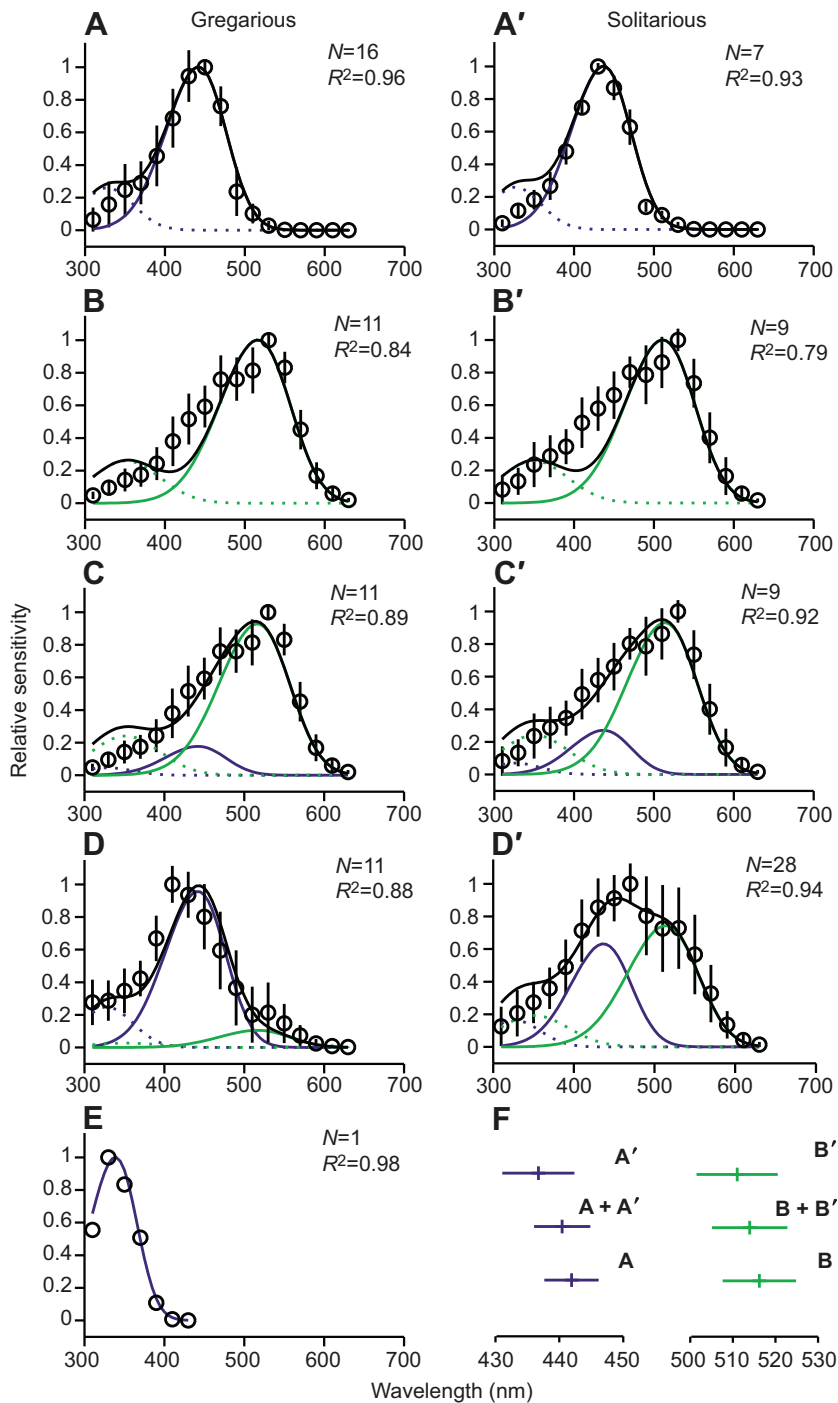
Fig. 6. Spectral sensitivity curves from different receptor types, based on intracellular recordings from gregarious and solitarious locusts. Data are sorted into DRA receptors (A,A′), non-DRA green (B,B′,C,C′) and non-DRA blue (D,D′) peaking receptors of gregarious (A–D) and solitarious (A′–D′) locusts. Open circles mark relative absorbances, averaged across N receptors and normalized to the value at the dominant peak wavelength (error bars: s.d.). The continuous black lines show fits of visual pigment-absorbance templates (see text). The goodness of fits is indicated by R^2 values. The continuous (dashed) lines in green and blue illustrate the fits' sub-templates for the α- (β-) bands of 'blue' and 'green' sensitive components, scaled to their relative contribution to the fit. Non-DRA green receptors are better described by inclusion of a blue component (C,C′) than by a green component alone (B,B′). (E) The relative sensitivity of a UV receptor could be measured only for one cell in a gregarious locust. (F) DRA blue and non-DRA green receptors do not differ between the two phases, as reflected by the 95% confidence intervals of their fitted dominant peak wavelengths. When pooling the data from gregarious and solitarious animals, peak absorbances of 441 nm (blue) and 514 nm (green) were obtained.

slightly smaller distal photoreceptor R7, and two proximal photoreceptors R1 and R4. This organization is reflected by opsin gene expression. In the main eye, receptors R2, R3, R5, R6 and R8 co-express Lo2 and Lo1, favouring a role in colour-blind motion detection, intensity coding and vision at low light levels. In contrast, the distal photoreceptor R7 expressing Lo2 or LoUV together with the two proximal photoreceptors R1 and R4 expressing Lo1 may constitute a trichromatic colour vision system operating at high light intensities. Behavioural studies supporting this hypothesis, however, are still missing. The two types of ommatidia differing in spectral types of R7 were stochastically distributed throughout the main eye without showing a dorsal–ventral gradient. Randomly distributed heterogeneous ommatidia were also found in the main retina of

honeybees (Wakakuwa et al., 2005) and the Japanese yellow swallowtail and monarch butterflies (Arikawa, 2003; Sauman et al., 2005). However, in some other Lepidoptera (e.g. Sison-Mangus et al., 2006; Awata et al., 2010), Diptera (e.g. Hu et al., 2011) and the two-spotted cricket (Henze et al., 2012), a dorsal–ventral gradient or regionalization was found with higher expression of long-wavelength opsins in ventral eye regions.

Spectral sensitivity

The distribution of three opsins in the locust retina is matched by spectral sensitivity profiles of photoreceptors as determined in ERG and intracellular recordings. In addition to narrowly tuned blue receptors in the DRA, we found in the main retina a UV peaking cell,
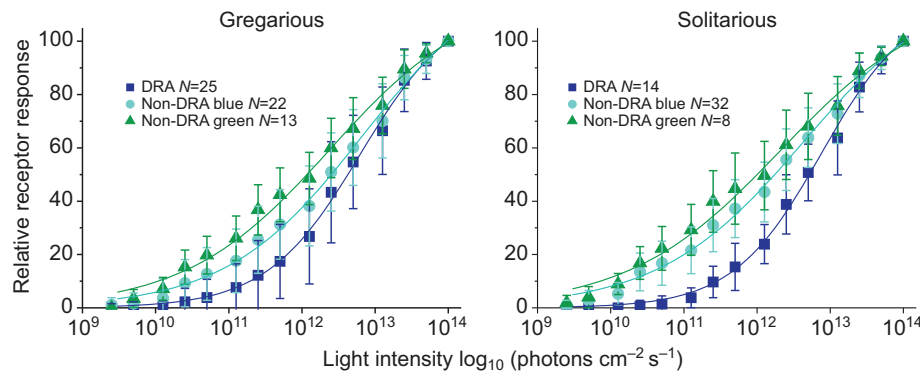
Fig. 7. Mean (±s.d.) relative V–log I curves from different receptor types of both locust phases. Data from DRA receptors (blue squares), non-DRA blue receptors (light blue circles), and non-DRA green receptors (green triangles) are compared. In both phases, the V–log I curves from DRA receptors are shifted to higher light intensities (high K) and are steeper than the non-DRA curves.

broadly sensitive blue peaking photoreceptors with shoulders of variable amplitude in the green, and photoreceptors with peak sensitivities in the green with a shoulder in the blue range (Fig. 6). Visual pigment template fits suggest that both the blue and green peaking photoreceptors contain a mixture of Lo1 and Lo2 opsins, albeit at different ratios. Narrowly tuned blue peaking receptors were not encountered in the main retina, suggesting that recordings from the Lo2 (blue opsin)-expressing photoreceptor R7 were not successful. Likewise, no narrowly tuned green receptors were found in the main retina, suggesting that recordings from the green opsin-expressing proximal photoreceptors were not successful. Broadband blue and green receptors have also been found in the compound eye of the migratory locust *L. migratoria* (Bennett et al., 1967; Vishnevskaya et al., 1986). Bennett et al. (Bennett et al., 1967) found considerable variation in the relative amplitude of green and blue peaks among different recorded cells and concluded that these locust receptors probably contain more than one opsin at different concentrations. This conclusion has long been obscured by the 'one cell-one pigment' dogma that has developed in recent years (Stavenga and Arikawa, 2008). The present study provides the first molecular as well as physiological evidence to support the conclusion of Bennett et al. (Bennett et al., 1967) after almost half a century.

A trichromatic set of UV, blue and green receptors is the most common state in insects (Briscoe and Chittka, 2001), whereas receptors containing more than one opsin have been reported only recently (Kitamoto et al., 1998; Arikawa et al., 2003; Mazzoni et al., 2008; Awata et al., 2010; Hu et al., 2011; Ogawa et al., 2012). Whereas in most cases two opsins of similar absorption spectra are co-expressed, combinations of UV and blue opsins have been

reported in the mosquito *Aedes* and the butterfly *Parnassius* (Awata et al., 2010; Hu et al., 2011). The co-expression of blue and green opsins in five out of eight photoreceptors per ommatidium (which results in broad spectral sensitivity curves) may be an adaptation to low light conditions. Blue light around 460 nm, matching the ERG spectral peak sensitivity in the dorsal eye, is dominant in sky light at dusk (Lythgoe, 1979).

In many insect species ventral eye regions are more sensitive to longer wavelengths (Awata et al., 2010). ERG recordings indicate that this is also the case for *S. gregaria*, especially in solitarious animals. In contrast, a dorsal–ventral gradient was not found in the pattern of opsin gene expression, but because *in situ* hybridization may not precisely reflect quantitative gene expression levels, it is conceivable that a dorsal–ventral gradient of Lo1/Lo2 ratio in R2, R3, R5, R6 and R8 does exist. High green sensitivity in ventral eye regions is probably linked to the detection of vegetation that reflects more green than UV (Schwind, 1983) or to the detection of the horizon (Stange, 1981). Behavioural experiments on ants, likewise, imply a functional regionalization of the eye in the DRA, DA and VA related to orientation tasks (Wehner, 1982; Fent, 1985).

Explanations for the high UV sensitivity in the VA of gregarious animals (Fig. 3) remain speculative. The amount of expressed UV opsin as well as increased UV receptor length and cross-section might account for the high UV sensitivity, but none of these possible factors has been examined.

V–log I curves

Higher K values imply that DRA receptors require more photons to be equally excited than non-DRA receptors, which therefore makes
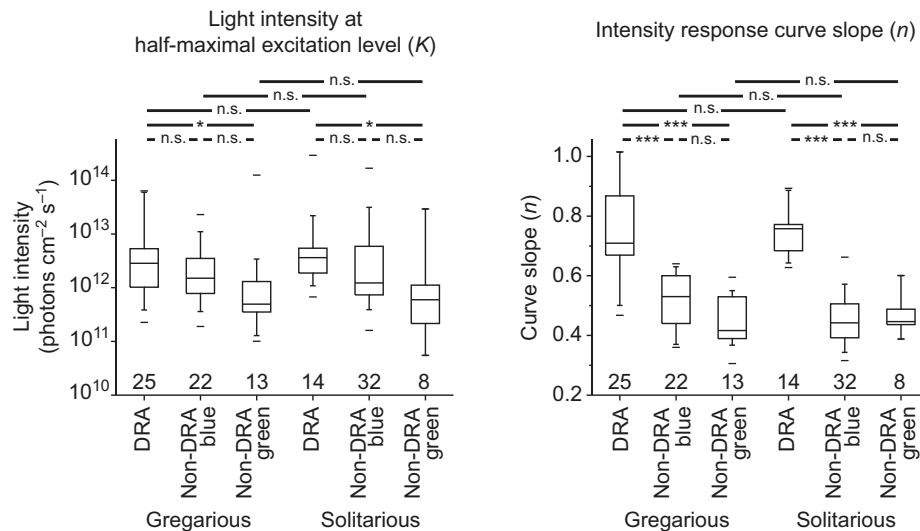
Fig. 8. Box plot diagrams comparing K and n values from different receptor types and eye regions in both locust phases. Significant differences were found for K values between DRA blue and non-DRA green receptors and for n values between DRA and non-DRA receptors (Kruskal–Wallis tests for K and one-way ANOVA with following Scheffé *post hoc* analysis for n; n.s., not significant; *$P<0.05$, ***$P<0.001$).
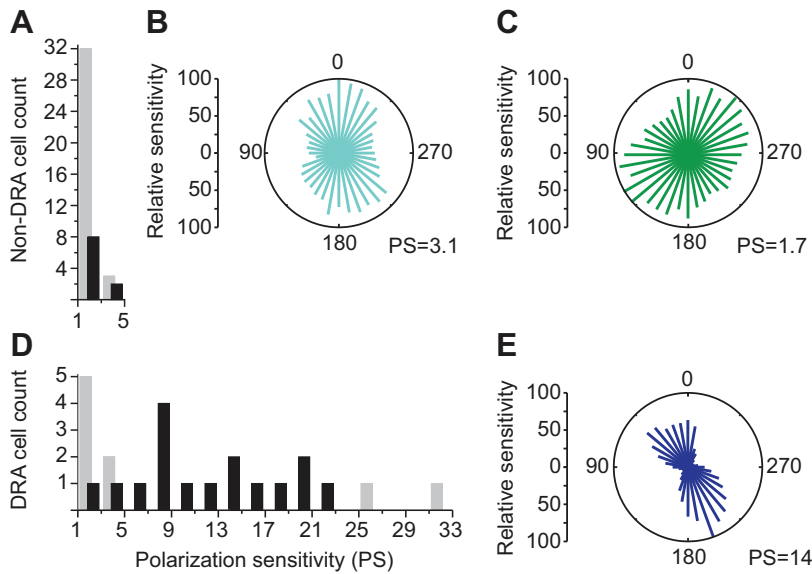
Fig. 9. Polarization sensitivities of photoreceptors in the DRA and main eye of gregarious and solitarious locusts. (A,D) Histograms of PS values. Data from gregarious locusts are shown in black, data from solitarious locusts in light grey. (B,C) Circular plots of POL responses of a non-DRA blue receptor (B) and a non-DRA green receptor (C). (E) Circular plot of POL responses of a blue receptor in the DRA.

them less sensitive. The reason for this condition might be the short rhabdom of DRA compared with non-DRA ommatidia (Wilson et al., 1978; Homberg and Paech, 2002). Two considerations, however, suggest that DRA receptors might actually be more sensitive. Firstly, owing to larger acceptance angles, DRA receptors are likely to collect more photons than non-DRA receptors with small visual fields (Zufall et al., 1989; Labhart et al., 1984). Thus DRA receptors may need more photons from a point light source to be excited than non-DRA receptors, but under a wide field stimulus, like the sky, they would actually collect more photons. Anatomical data suggest that this is the case in the locust (Homberg and Paech, 2002; Wilson

et al., 1978). Secondly, DRA receptors have microvilli with parallel orientation, being more sensitive to E-vectors in parallel to the microvilli than to orthogonal E-vectors. V–$\log I$ curves were recorded while stimulating with unpolarized light. Because non parallel E-vector orientations are less effectively detected by DRA receptors they would appear to be less sensitive to unpolarized light than non-DRA receptors under otherwise similar conditions.

The exponential slope of the V–$\log I$ curve, n, determines the sensitivity of a photoreceptor to differences in light intensity. The steeper slope (larger n) in DRA versus non-DRA receptors indicates a smaller total response range in DRA receptors than in non-DRA
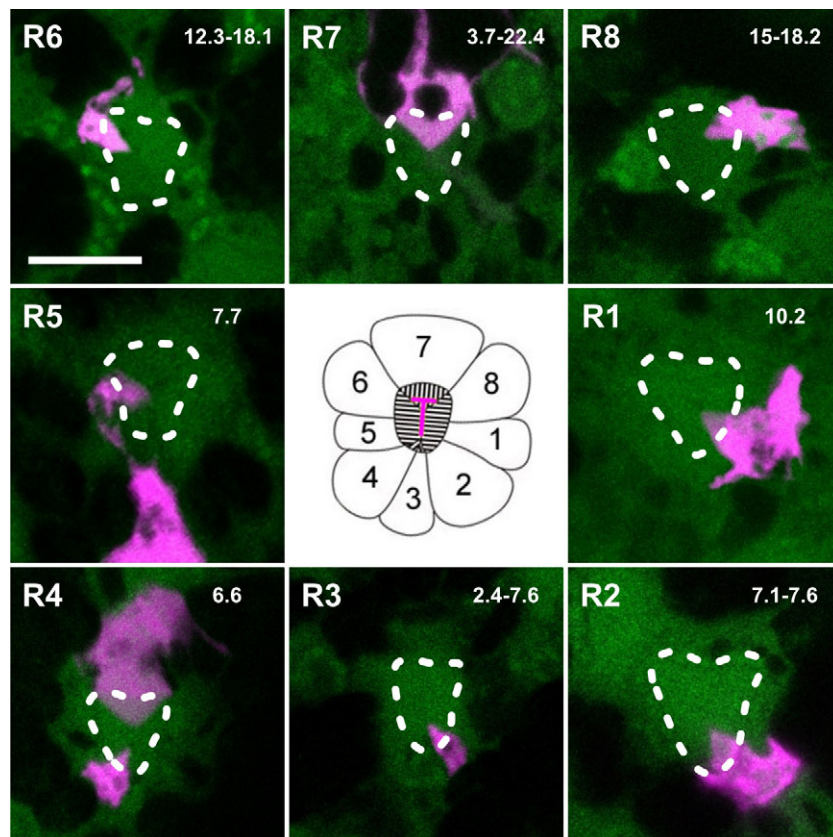
Fig. 10. Confocal laser scanning images of stained single DRA receptor cells of gregarious locusts. Stained cells (magenta) from the right eye (R3, R4, R7) are shown as mirror images to correspond to data from the left eye. Numbers in the upper right of the images indicate range of recorded PS values in this cell type. Only R4 could not be labelled individually. The Φ_{max} orientation of this recording showed best fit to the microvilli orientation of the R4 cell, hence this cell is considered to be recorded from. Additional staining in the image of R5 belongs to an R7 from a neighbouring ommatidium. Scale bar, 5 µm.

receptors. This may contribute to the narrow intensity-dependent response range found in polarization-sensitive interneurons in crickets (Labhart, 1988) and locusts (Kinoshita et al., 2007), which above a certain light level signal E-vector orientation independent of light intensity.

Differences in the slope of V–log I curves have also been found between light- and dark-adapted photoreceptors in *L. migratoria* and other insects (Matić and Laughlin, 1981). *L. migratoria* receptor response curves were steeper in the light-adapted state with n up to 1, than in the dark-adapted state with n up to 0.6, which corresponds to values in the desert locust (Fig. 7).

Polarization sensitivity

High PS values (>4) were only found in the DRA, supporting ultrastructural (Homberg and Paech, 2002) and behavioural evidence (Mappes and Homberg, 2004) for the role of the DRA in celestial E-vector detection. Apparently all DRA photoreceptors contribute to high polarization sensitivity including receptors R3 and R4 which, based upon irregularities in microvillar alignment, were hitherto assumed to have low polarization sensitivity (Homberg and Paech, 2002). PS values below 3 measured in some recordings might, instead, result from damaged receptor cells during the experimental procedure. The expression of Lo2 (blue) opsin and peak sensitivity in the blue (441 nm) are consistent with data from Eggers and Gewecke (Eggers and Gewecke, 1993) but the presence of UV receptors in the DRA as reported by the same authors could not be confirmed.

The spectral sensitivity of polarization-sensitive photoreceptors differs considerably among different insect species. POL sensitivity in the green spectrum has been linked to greenish light conditions under tree canopies (Hegedüs et al., 2006). UV and blue POL sensitivity is more likely to be an adaptation to conditions under the free sky. Several authors have discussed that POL vision in the blue instead of the UV might be advantageous for insects active under crepuscular conditions (Labhart et al., 1984; Zufall et al., 1989; Horváth and Varjú, 2004). The sky polarization pattern is most stable in the UV and also reliable under cloudy conditions (Barta and Horváth, 2004). However, overall sky radiance is weaker in the UV than at longer wavelengths (Lythgoe, 1979; Johnsen et al., 2006), favouring blue receptors for animals that navigate at low light levels. POL vision of solitarious desert locusts follows this logic, and the phase change to the day-active gregarious phase might not have altered the spectral sensitivity of the DRA.

Phase-dependent differences in spectral sensitivity

Various differences in the visual system of solitarious and gregarious locusts have been reported, including differences in eye size, number of ommatidia and sensitivity to motion stimuli (Matheson et al., 2004; Ott and Rogers, 2010; Rogers et al., 2010; Gaten et al., 2012), while polarization-sensitive interneurons were not noticeably affected by locust phase (el Jundi and Homberg, 2012). Here we show differences in photoreceptor spectral sensitivities, particularly in the ventral eye as revealed by ERG recordings and in peak wavelength of blue peaking receptors found in intracellular recordings. Judged from the *in situ* hybridization data, the high UV sensitivity in the ventral eye of gregarious animals, measured by ERGs, cannot be explained by changing receptor occurrences but may result from differences in rhabdomere lengths and cross-sections in different eye regions which were not studied here. In addition, differences in the relative concentrations of Lo1/Lo2 opsins may underlie not only the sensitivity differences in the blue–green range between dorsal and ventral eye regions but also the differences in the sensitivities between the phases.

Provided that the same opsin genes are expressed in solitarious and gregarious animals, the visual pigment template fits indicate that especially in blue peaking receptors, the contributions of Lo1 and Lo2 opsins are strikingly different between the two phases, resulting in a considerable shift of absorption curves to longer wavelengths in solitarious animals (Fig. 6D,D′). An alternative explanation for these differences may be circadian rather than phase-dependent changes, because gregarious locusts were tested during the day and solitarious locusts in their activity phase during the night. Diurnal and circadian changes in photoreceptor sensitivity and microvillar membrane turnover have been detected in various insect species, including locusts (e.g. Horridge et al., 1981; Fleissner, 1982). Light-induced movement of visual pigment and circadian changes in visual pigment levels have been demonstrated in mosquito photoreceptors (Hu et al., 2012). Differing secondary green sensitivity in the locust might, therefore, not be phase dependent, but daytime dependent. If so, however, circadian effects would have to be restricted to blue and green peaking receptors of the main eye, because we did not detect corresponding differences in the DRA.

MATERIALS AND METHODS

Animals

Adult male and female locusts (*Schistocerca gregaria*) were obtained from breeding colonies at the University of Marburg. Gregarious animals were kept crowded at 12 h:12 h light:dark cycle, 28°C room temperature and 50% relative humidity. Solitarious animals were reared individually in small boxes at 12 h:12 h light:dark cycle, 26.5°C and 60% relative humidity following the conditions established by Roessingh et al. (Roessingh et al., 1993). In particular, no visual, olfactory and mechanical contact occurred between individuals. Animals used for experiments had been reared in solitarious conditions for at least three generations. Typical morphological characteristics such as body colouration and size (Simpson et al., 1999; el Jundi and Homberg, 2012) served as indicators for the solitarious phase of the animals. Only locusts at least 1 week after imaginal moult were used for experiments.

Molecular cloning

Poly-A RNA was extracted from the eyes of gregarious animals using a QuickPrep micro mRNA purification kit (GE Healthcare, Uppsala, Sweden). To amplify fragments of cDNAs encoding opsins of the UV class, we carried out RT-PCR using degenerate primers designed based on consensus sequences of short wavelength (UV and blue) absorbing opsins of insects identified so far. The full-length cDNAs were obtained by the 5′- and 3′-RACE (rapid amplification of cDNA ends) methods. Both PCR and RACE products were purified, cloned using a TOPO TA cloning kit (Invitrogen, Carlsbad, CA, USA) and sequenced using ABI3130xl and BigDye terminator v1.1 (Applied Biosystems, Warrington, UK). The obtained sequences were aligned with others and processed for phylogenetic analysis by the neighbour-joining (NJ) protocols in MEGA 5.2.2 software with a bootstrap of 1000 replicates and a Poisson model for amino acid substitution.

In situ hybridization

We performed double-targeted *in situ* hybridization on paraffin sections as described previously (Awata et al., 2010). Digoxigenin and biotin labelled RNA probes were synthesized from linearized plasmids carrying the partial sequences of coding regions (Lo1: 1003 bp; Lo2: 948 bp; LoUV: 929 bp) of the mRNAs encoding the Lo1, Lo2 and LoUV opsins by *in vitro* transcription.

The compound eyes of gregarious *S. gregaria* were fixed in 4% paraformaldehyde in 0.1 mol l⁻¹ sodium phosphate buffer (pH 7.2) and embedded in paraffin. The paraffin-embedded eyes were sectioned at 6 μm thickness with a rotary microtome. The sections were first de-paraffinized and treated with hybridization solution at 45°C containing 0.5 μg ml⁻¹ of the mixture of two cRNA probes, one labelled with digoxigenin and another labelled with biotin, which were hybridized to different opsin mRNA. After the hybridization process, the digoxigenin-labelled probes were first detected

using anti-digoxigenin antibody conjugated to alkaline phosphatase and then visualized using 4-nitroblue-tetrazolium chloride and 5-bromo-4-chloro-3-indolyl phosphate. The sections were briefly washed and treated with 100 mmol l^{-1} glycine solution (pH 2.2) to remove the unbound anti-digoxigenin antibody. The hybridized biotin-labelled probes were detected using streptavidin-alkaline phosphatase conjugate and visualized using Fast Red (Roche, Mannheim, Germany). The numbering of photoreceptor cells in ommatidia of the ordinary eye region corresponds to that used for *L. migratoria* (Wilson et al., 1978).

Electrophysiology and visual stimulation

Animals were immobilized by cutting off their legs and wings. They were mounted with wax to a metal holder and placed in the centre of an electrophysiological recording set-up. Experiments on gregarious animals were performed during the day and experiments on solitarious animals during the night. Photoreceptors were studied through ERG and intracellular recordings. For differential ERG recordings, a silver wire electrode (diameter 75 μm, Teflon coated; Science Products, Hofheim, Germany) was inserted into each eye. A third silver wire in the head capsule served as reference electrode. Responses were amplified 100× by an AC pre-amplifier (P55, Grass-Telefactor, West Warwick, RI, USA). Light stimuli were presented to one eye through the end of a light guide. To detect regional differences in spectral sensitivity, parts of the eye were covered with black paint (Decormatt Acryl, Marabu, Bietigheim-Bissingen, Germany) leaving out either the dorsal rim area (DRA), the dorsal area (DA), or the ventral area (VA) of the main retina.

For intracellular recordings, glass microelectrodes were drawn from borosilicate capillaries (inner diameter, 0.75 mm; outer diameter, 1.5 mm; Hilgenberg, Malsfeld, Germany) using a Flaming/Brown horizontal puller (P-97, Sutter Instruments, Novato, Canada). Electrode tips were filled with 4% neurobiotin (Vector Laboratories, Peterborough, UK) in 1 mol l^{-1} KCl and backed up with 3 mol l^{-1} KCl. Electrodes had resistances of 30–100 MΩ and were inserted into the region of interest through a small hole cut into the cornea. A silver wire inserted into the head of the locust served as the indifferent electrode. Signals were amplified 10× (BA-01X, NPI, Tamm, Germany), digitized at a sampling rate of 2 kHz (Digidata 1322A, Axon Instruments, Union City, CA, USA), and stored on a PC using Spike2 (Cambridge Electronic Design, Cambridge, UK) or pCLAMP10 software (Molecular Devices, Sunnyvale, CA, USA).

Monochromatic light stimuli were provided by a 75 W xenon arc lamp (L.O.T.-Oriel, Darmstadt, Germany). Light passed a monochromator (Omni-λ150, LOT-Oriel; bandwidth 10 nm), a neutral density wedge, adjusted to each wavelength to guarantee equal photon flux, and a set of filter wheels (Lambda 10-3, Sutter Instruments) containing neutral density filters (quartz glass; 2×50%, 10%, 1%, 0.1% and 0.01% transmission; L.O.T.-Oriel). Light was finally directed via a light guide (quartz glass; Schott, Mainz, Germany) positioned close to the locust's eye (angular extent at the eye 3 deg). A linear polarization filter (HNP'B, Polaroid, Cambridge, UK) could be moved in front of the light guide. The light guide and polarizer were fixed to a perimeter arm and could thus be moved around the locust with its head in the centre. The monochromator, wedge, filter wheels and polarizer were controlled via custom-programmed PC software.

Continuous flashes of white light were presented to the animal (duration 200 ms, pause 1 s), while advancing the electrode through the tissue. Penetration of a photoreceptor cell was indicated by a characteristic drop in baseline voltage followed by graded depolarizations in response to the light flashes. After penetrating a cell, the light guide was moved to the centre of the receptor's visual field, indicated by maximum response amplitude. To test for spectral response, a series of 17 monochromatic light flashes of equal quantal flux were given, starting from 310 nm to 630 nm in 20 nm steps. In some cases this procedure was repeated in the opposite direction from 630 to 310 nm. Light intensity was adjusted individually for each spectral test series to elicit response amplitudes within the estimated dynamic range of the intensity response curve. Light flash duration was 500 ms. Pauses between the flashes were 7 or 10 s in intracellular recordings and 10 or 30 s in extracellular ERG recordings.

For testing polarization response the polarizer was moved in front of the light guide and was rotated in 10 deg steps through 180 or 360 deg. While the polarizer was stationary a light flash of the most sensitive wavelength was presented (duration 500 ms, pause 10 or 15 s). As in the spectral test, light intensity was chosen to elicit response amplitudes within the dynamic range of the intensity response curve. Before starting the stimulus series, two flashes of polarized light (0 deg) were given to eliminate adaptation effects. All experiments were performed in a darkened room.

Intensity response curves (*V*–log *I*) were obtained by presenting flashes of the most effective stimulus wavelength for the penetrated cell in 14 steps of increasing intensities over 4.6 log units. Maximum light intensity in the UV range (310–350 nm) was 2.8×10^{13} photons cm^{-2} s^{-1}, in the blue range (410–450 nm) 3.9×10^{13} photons cm^{-2} s^{-1}, and in the green range (510–530 nm) 2.8×10^{13} photons cm^{-2} s^{-1}. By using the *V*–log *I* curve, we converted the spectral and polarization responses into spectral and polarization sensitivities. For the procedure, see Arikawa et al. (Arikawa et al., 2003).

In later experiments, the spectral test was shortened to reduce recording time. Instead of 17 light flashes with different wavelengths, only three light flashes were presented to the locust which fitted the mean maximum sensitivities of the receptor types found so far (350, 430 and 530 nm). The wavelength at which the highest response amplitude occurred was considered to represent the maximum sensitivity of the receptor. Further intensity response curves and tests for polarization sensitivity were performed with this wavelength. For histological evaluation neurobiotin was, finally, injected iontophoretically into the receptor cell with constant depolarized current (0.5–2 nA for 1–3 min).

Data analysis

Only recordings with a maximum response amplitude of at least 25 mV were used for data evaluation (except for a single UV cell in Fig. 6). A 20 mV limit was set for single spectral recordings with the aim to gain information on peak sensitivity. Other criteria were a stable baseline during recordings and the absence of ERG artifacts (see Fig. 4A–C). Recording files were transferred to Spike2 software for measuring voltage amplitudes. To calculate relative sensitivities of the responses, Naka–Rushton functions:

$$V/V_{max} = I^n/(I^n + K^n),\tag{1}$$

with *I* the stimulus intensity, *V* the response amplitude at a certain stimulus, V_{max} the maximum response amplitude, *K* the stimulus intensity causing 50% of V_{max} and *n* the exponential slope, were fitted to data from the *V*–log *I* curves using Origin6 software (Microcal Software, Northampton, MA, USA).

Polarization sensitivity (PS) of photoreceptors is defined as:

$$PS = S_{max}/S_{min},\tag{2}$$

where S_{max} and S_{min} are the relative sensitivities to E-vectors exciting the receptor maximally and minimally, respectively (Labhart, 1980).

Data were tested for normal distribution using the Shapiro–Wilk test and for homogeneity of variance with the Levene test using SPSS software (version 19). Multiple comparisons of normally distributed data were performed with one-way ANOVA (combined with Scheffé *post hoc* analysis). Kruskal–Wallis tests were applied to non-normally distributed data.

Visual pigment absorption templates (Govardovskii et al., 2000) were fitted to the absorbance spectra from the intracellularly recorded photoreceptors using the curve fitting toolbox of MATLAB (MathWorks, Natick, MA, USA). In all fits, the amplitude of the β-band of visual pigment was kept at a fixed relative value of 0.26, and linear relationships between λ_{max} and both the bandwidth and amplitude of the β-band were assumed (Govardovskii et al., 2000).

Histology

Retinae and optic lobes with neurobiotin-injected cells were dissected and fixed overnight in neurobiotin fixative (4% paraformaldehyde, 0.25% glutaraldehyde, 2% saturated picric acid, in 0.1 mol l^{-1} phosphate buffer) at 4°C. Following rinses in 0.1 mol l^{-1} phosphate-buffered saline (PBS, pH 7.4) for 4×15 min the lobes were pre-incubated with 5% normal goat serum (NGS) in PBS for 3 h at room temperature, and subsequently for 2–3 days at 4°C in streptavidin-Cy3 conjugate (1:1000) and a primary antibody against *Drosophila* synapsin (1:30) (see Klagges et al., 1996) in 0.1 mol l^{-1}

PBS/0.3% Triton X-100/1% NGS. After rinsing in 0.1 mol l⁻¹ PBS + 0.3% Triton X-100 for 4×15 min, the preparations were incubated in secondary antibody (0.8% goat anti mouse-Cy5, 0.1% streptavidin-Cy3 and 1% NGS in 0.1 mol l⁻¹ PBS + 0.3% Triton X-100) at 4°C for 2 days. Retinae/optic lobes were subsequently dehydrated through an ascending ethanol series, transferred to propylene oxide and embedded in soft Spurr's resin (Spurr, 1969). Cross-sections of the ommatidium with the stained photoreceptor cell were cut at 10 μm with a rotary microtome (Leitz, Wetzlar, Germany).

Sections were embedded in Permount (Fisher Scientific, Pittsburgh, PA, USA) and were scanned with a confocal laser scanning microscope (TCS SP5, Leica Microsystems, Wetzlar, Germany), using a 10× objective (HC PL APO 10×/0.4 Imm Corr CS; Leica, Bensheim, Germany) for overviews and a 63× objective (HCX PL APO 63×/1.32 OIL PH 3CS; Leica) for details (scanning intervals 1–2 μm). Fluorescence of stained cells was detected with a He/Ne laser (excitation wavelength 543 nm for Cy3) or an Ar/Kr laser (excitation wavelength 647 nm for Cy5). Images were processed in CLSM imaging software (LAS AF v. 2.2.1 build 4842, Leica, Mannheim, Germany) and graphic software (CorelDRAW X3, Corel). From the time of incubation with the fluorophores, the preparations were kept in the dark as much as possible.

References

Arikawa, K. (2003). Spectral organization of the eye of a butterfly, *Papilio*. *J. Comp. Physiol. A* **189**, 791-800.

Arikawa, K., Mizuno, S., Kinoshita, M. and Stavenga, D. G. (2003). Coexpression of two visual pigments in a photoreceptor causes an abnormally broad spectral sensitivity in the eye of the butterfly *Papilio xuthus*. *J. Neurosci.* **23**, 4527-4532.

Awata, H., Matsushita, A., Wakakuwa, M. and Arikawa, K. (2010). Eyes with basic dorsal and specific ventral regions in the glacial Apollo, *Parnassius glacialis* (Papilionidae). *J. Exp. Biol.* **213**, 4023-4029.

Barta, A. and Horváth, G. (2004). Why is it advantageous for animals to detect celestial polarization in the ultraviolet? Skylight polarization under clouds and canopies is strongest in the UV. *J. Theor. Biol.* **226**, 429-437.

Bennett, R. R., Tunstall, J. and Horridge, G. A. (1967). Spectral sensitivity of single retinula cells of the locust. *Z. Vgl. Physiol.* **55**, 195-206.

Briscoe, A. D. and Chittka, L. (2001). The evolution of color vision in insects. *Annu. Rev. Entomol.* **46**, 471-510.

Brunner, D. and Labhart, T. (1987). Behavioural evidence for polarization vision in crickets. *Physiol. Entomol.* **12**, 1-10.

Dacke, M., Nordström, P. and Scholtz, C. H. (2003). Twilight orientation to polarised light in the crepuscular dung beetle *Scarabaeus zambesianus*. *J. Exp. Biol.* **206**, 1535-1543.

Dacke, M., Byrne, M. J., Baird, E., Scholtz, C. H. and Warrant, E. J. (2011). How dim is dim? Precision of the celestial compass in moonlight and sunlight. *Philos. Trans. R. Soc. B* **366**, 697-702.

Eggers, A. and Gewecke, M. (1993). The dorsal rim area of the compound eye and polarization vision in the desert locust (*Schistocerca gregaria*). In *Sensory Systems of Arthropods* (ed. K. Wiese, F. G. Gribakin, A. V. Popov and G. Renninger), pp. 101-109. Basel: Birkhäuser.

el Jundi, B. and Homberg, U. (2012). Receptive field properties and intensity-response functions of polarization-sensitive neurons of the optic tubercle in gregarious and solitarious locusts. *J. Neurophysiol.* **108**, 1695-1710.

Fent, K. (1985). *Himmelsorientierung bei der Wüstenameise Cataglyphis bicolor: Bedeutung von Komplexaugen und Ocellen*. Dissertation, University of Zurich, Switzerland.

Fleissner, G. (1982). Isolation of an insect circadian clock. *J. Comp. Physiol. A* **149**, 311-316.

Gaten, E., Huston, S. J., Dowse, H. B. and Matheson, T. (2012). Solitary and gregarious locusts differ in circadian rhythmicity of a visual output neuron. *J. Biol. Rhythms* **27**, 196-205.

Govardovskii, V. I., Fyhrquist, N., Reuter, T., Kuzmin, D. G. and Donner, K. (2000). In search of the visual pigment template. *Vis. Neurosci.* **17**, 509-528.

Hegedüs, R., Horváth, A. and Horváth, G. (2006). Why do dusk-active cockchafers detect polarization in the green? The polarization vision in *Melolontha melolontha* is tuned to the high polarized intensity of downwelling light under canopies during sunset. *J. Theor. Biol.* **238**, 230-244.

Heinze, S. and Homberg, U. (2007). Maplike representation of celestial E-vector orientations in the brain of an insect. *Science* **315**, 995-997.

Heinze, S., Gotthardt, S. and Homberg, U. (2009). Transformation of polarized light information in the central complex of the locust. *J. Neurosci.* **29**, 11783-11793.

Henze, M. J., Dannenhauer, K., Kohler, M., Labhart, T. and Gesemann, M. (2012). Opsin evolution and expression in arthropod compound eyes and ocelli: insights from the cricket *Gryllus bimaculatus*. *BMC Evol. Biol.* **12**, 163.

Homberg, U. and el Jundi, B. (2014). Polarization vision in arthropods. In *The New Visual Neurosciences* (ed. J. S. Werner and L. M. Chalupa), pp. 1207-1217. Cambridge, MA: MIT Press.

Homberg, U., Heinze, S., Pfeiffer, K., Kinoshita, M. and el Jundi, B. (2011). Central neural coding of sky polarization in insects. *Philos. Trans. R. Soc. B* **366**, 680-687.

Homberg, U. and Paech, A. (2002). Ultrastructure and orientation of ommatidia in the dorsal rim area of the locust compound eye. *Arthropod Struct. Dev.* **30**, 271-280.

Horridge, G. A., Duniec, J. and Marčelja, L. (1981). A 24-hour cycle in single locust and mantis photoreceptors. *J. Exp. Biol.* **91**, 307-322.

Horváth, G. and Varjú, D. (2004). *Polarized Light in Animal Vision: Polarization Patterns in Nature*. Heidelberg: Springer.

Hu, X., Leming, M. T., Metoxen, A. J., Whaley, M. A. and O'Tousa, J. E. (2012). Light-mediated control of rhodopsin movement in mosquito photoreceptors. *J. Neurosci.* **32**, 13661-13667.

Hu, X., Whaley, M. A., Stein, M. M., Mitchell, B. E. and O'Tousa, J. E. (2011). Coexpression of spectrally distinct rhodopsins in *Aedes aegypti* R7 photoreceptors. *PLoS ONE* **6**, e23121.

Johnsen, S., Kelber, A., Warrant, E., Sweeney, A. M., Widder, E. A., Lee, R. L., Jr and Hernández-Andrés, J. (2006). Crepuscular and nocturnal illumination and its effects on color perception by the nocturnal hawkmoth *Deilephila elpenor*. *J. Exp. Biol.* **209**, 789-800.

Kennedy, J. S. (1951). The migration of the desert locust (*Schistocerca gregaria* Forsk). I. The behaviour of swarms. II. A theory of long-range migrations. *Phil. Trans. R. Soc. B* **235**, 163-290.

Kinoshita, M., Pfeiffer, K. and Homberg, U. (2007). Spectral properties of identified polarized-light sensitive interneurons in the brain of the desert locust *Schistocerca gregaria*. *J. Exp. Biol.* **210**, 1350-1361.

Kitamoto, J., Sakamoto, K., Ozaki, K., Mishina, Y. and Arikawa, K. (1998). Two visual pigments in a single photoreceptor cell: identification and histological localization of three mRNAs encoding visual pigment opsins in the retina of the butterfly *Papilio xuthus*. *J. Exp. Biol.* **201**, 1255-1261.

Klagges, B. R., Heimbeck, G., Godenschwege, T. A., Hofbauer, A., Pflugfelder, G. O., Reifegerste, R., Reisch, D., Schaupp, M., Buchner, S. and Buchner, E. (1996). Invertebrate synapsins: a single gene codes for several isoforms in *Drosophila*. *J. Neurosci.* **16**, 3154-3165.

Labhart, T. (1980). Specialized photoreceptors at the dorsal rim of the honeybee's compound eye: polarizational and angular sensitivity. *J. Comp. Physiol. A* **141**, 19-30.

Labhart, T. (1988). Polarization-opponent interneurons in the insect visual system. *Nature* **331**, 435-437.

Labhart, T., Hodel, B. and Valenzuela, I. (1984). The physiology of the cricket's compound eye with particular reference to the anatomically specialized dorsal rim area. *J. Comp. Physiol. A* **155**, 289-296.

Labhart, T. and Meyer, E. P. (1999). Detectors for polarized skylight in insects: a survey of ommatidial specializations in the dorsal rim area of the compound eye. *Microsc. Res. Tech.* **47**, 368-379.

Lythgoe, J. N. (1979). *The Ecology of Vision*. Oxford: Clarendon Press.

Mappes, M. and Homberg, U. (2004). Behavioral analysis of polarization vision in tethered flying locusts. *J. Comp. Physiol. A* **190**, 61-68.

Matheson, T., Rogers, S. M. and Krapp, H. G. (2004). Plasticity in the visual system is correlated with a change in lifestyle of solitarious and gregarious locusts. *J. Neurophysiol.* **91**, 1-12.

Matić, T. and Laughlin, S. B. (1981). Changes in the intensity-response function of an insect's photoreceptors due to light adaptation. *J. Comp. Physiol. A* **145**, 169-177.

Mazzoni, E. O., Celik, A., Wernet, M. F., Vasiliauskas, D., Johnston, R. J., Cook, T. A., Pichaud, F. and Desplan, C. (2008). Iroquois complex genes induce co-expression of rhodopsins in *Drosophila*. *PLoS Biol.* **6**, e97.

Ogawa, Y., Awata, H., Wakakuwa, M., Kinoshita, M., Stavenga, D. G. and Arikawa, K. (2012). Coexpression of three middle wavelength-absorbing visual pigments in sexually dimorphic photoreceptors of the butterfly *Colias erate*. *J. Comp. Physiol. A* **198**, 857-867.

Ott, S. R. and Rogers, S. M. (2010). Gregarious desert locusts have substantially larger brains with altered proportions compared with the solitarious phase. *Proc. Biol. Sci.* **277**, 3087-3096.

Pfeiffer, K. and Homberg, U. (2007). Coding of azimuthal directions via time-compensated combination of celestial compass cues. *Curr. Biol.* **17**, 960-965.

Reppert, S. M., Zhu, H. and White, R. H. (2004). Polarized light helps monarch butterflies navigate. *Curr. Biol.* **14**, 155-158.

Roessingh, P., Simpson, S. J. and James, S. (1993). Analysis of phase-related changes in behaviour of desert locust nymphs. *Proc. Biol. Sci.* **252**, 43-49.

Roffey, J. (1963). Observations on night flight in the desert locust (*Schistocerca gregaria* Forskål). *Anti-Locust Bull.* **39**, 1-32.

Roffey, J. and Magor, J. I. (2003). *Desert Locust Population Dynamics Parameters.* Desert locust technical series. Rome: Food and Agriculture organization (FAO) of the United Nations.

Rogers, S. M., Harston, G. W. J., Kilburn-Toppin, F., Matheson, T., Burrows, M., Gabbiani, F. and Krapp, H. G. (2010). Spatiotemporal receptive field properties of a looming-sensitive neuron in solitarious and gregarious phases of the desert locust. *J. Neurophysiol.* **103**, 779-792.

Sauman, I., Briscoe, A. D., Zhu, H., Shi, D., Froy, O., Stalleicken, J., Yuan, Q., Casselman, A. and Reppert, S. M. (2005). Connecting the navigational clock to sun compass input in monarch butterfly brain. *Neuron* **46**, 457-467.

Schwind, R. (1983). Zonation of the optical environment and zonation in the rhabdom structure within the eye of the backswimmer, *Notonecta glauca*. *Cell Tissue Res.* **232**, 53-63.

Simpson, S. J., McCafferey, A. R. and Hägele, B. (1999). A behavioural analysis of phase change in the desert locust. *Biol. Rev. Camb. Philos. Soc.* **74**, 461-480.

Sison-Mangus, M. P., Bernard, G. D., Lampel, J. and Briscoe, A. D. (2006). Beauty in the eye of the beholder: the two blue opsins of lycaenid butterflies and the opsin gene-driven evolution of sexually dimorphic eyes. *J. Exp. Biol.* **209**, 3079-3090.

Spurr, A. R. (1969). A low-viscosity epoxy resin embedding medium for electron microscopy. *J. Ultrastruct. Res.* **26**, 31-43.

Stange, G. (1981). The ocellar component of flight equilibrium control in dragonflies. *J. Comp. Physiol. A* **141**, 335-347.

Stavenga, D. G. and Arikawa, K. (2008). One rhodopsin per photoreceptor: Iro-C genes break the rule. *PLoS Biol.* **6**, e115.

Towner, P., Harris, P., Wolstenholme, A. J., Hill, C., Worm, K. and Gärtner, W. (1997). Primary structure of locust opsins: a speculative model which may account for ultraviolet wavelength light detection. *Vision Res.* **37**, 495-503.

Uvarov, B. (1966). *Grasshoppers and Locusts. A Handbook of General Acridology*. Cambridge: Cambridge University Press.

Vishnevskaya, T. M., Cherkasov, A. D. and Shura-Bura, T. M. (1986). Spectral sensitivity of photoreceptors in the compound eye of the locust. *Neurophysiology* **18**, 54-60.

von Frisch, K. (1949). Die Polarisation des Himmelslichtes als orientierender Faktor bei den Tänzen der Bienen. *Experientia* **5**, 142-148.

von Philipsborn, A. and Labhart, T. (1990). A behavioural study of polarization vision in the fly, *Musca domestica*. *J. Comp. Physiol. A* **167**, 737-743.

Wakakuwa, M., Kurasawa, M., Giurfa, M. and Arikawa, K. (2005). Spectral heterogeneity of honeybee ommatidia. *Naturwissenschaften* **92**, 464-467.

Waloff, Z. (1963). Field studies on solitary and transiens desert locusts in the Red Sea area. *Anti-Locust Bull.* **40**, 1-91.

Wehner, R. (1982). Himmelsnavigation bei Insekten: Neurophysiologie und Verhalten. *Neujahrsblatt Naturforsch. Ges. Zürich* **184**, 1-132.

Wehner, R. and Labhart, T. (2006). Polarisation vision. In *Invertebrate Vision* (ed. E. Warrant and D. E. Nilsson), pp. 291-348. Cambridge: Cambridge University Press.

Wehner, R. and Müller, M. (2006). The significance of direct sunlight and polarized skylight in the ant's celestial system of navigation. *Proc. Natl. Acad. Sci. USA* **103**, 12575-12579.

Weir, P. T. and Dickinson, M. H. (2012). Flying *Drosophila* orient to sky polarization. *Curr. Biol.* **22**, 21-27.

Wilson, M., Garrard, P. and McGinness, S. (1978). The unit structure of the locust compound eye. *Cell Tissue Res.* **195**, 205-226.

Zufall, F., Schmitt, M. and Menzel, R. (1989). Spectral and polarized light sensitivity of photoreceptors in the compound eye of the cricket (*Gryllus bimaculatus*). *J. Comp. Physiol. A* **164**, 597-608.